ARMA 18-1100

Random field realization and fracture simulation of rocks with angular bias for fracture strength

Garrard, J.M., Abedi, R., Clarke, P.L.
Department of Mechanical, Aerospace & Biomedical Engineering, The University of Tennessee Space Institute, TN, USA

ABSTRACT: Realistic fracture simulations in rock as a heterogeneous brittle material with significant inherent randomness require the use of models that incorporate its inhomogeneities and statistical variability. The high dependence of their fracture progress on microstructural defects results in wide scatter in their ultimate strength and the so-called size effect. This paper proposes an approach based on *statistical volume elements* (SVEs) to characterize rock fracture strength at the mesoscale. The use of SVEs ensures that the material randomness is maintained upon averaging of microscale features. Because the fracture strength varies not just spatially, but also by the angle of loading, this work includes angular variability to properly model a heterogeneous rock domain. Two different microcrack distributions, one angularly uniform and one angularly biased towards a specific angle, are used to show that implementing angle into the random field provides the most realistic fracture simulation. An adaptive *asynchronous spacetime discontinuous Galerkin* (aSDG) finite element method is used to perform the dynamic fracture simulations.
Acknowledgments: The authors gratefully acknowledge partial support for this work via the U.S. National Science Foundation (NSF), CMMI - Mechanics of Materials and Structures (MoMS) program grant number 1538332 and CCF - Scalable Parallelism in the Extreme (SPX) program grant number 1725555.

1 INTRODUCTION

The behavior of quasi-brittle materials, such as rock, under load is influenced by heterogeneity at several scales. In the macroscale, different rock types, layers, and faults define the overall system characteristics. At the microscale, networks of microcracks can lead to a non-homogeneous fracture behavior under loading depending on the load angle. These cracks and microstructural defects influence the material's peek and post-instability response, as shown in [Kozicki and Tejchman, 2007, Yin et al., 2008] and fracture patterns even under the same loading and geometry settings [Al-Ostaz and Jasiuk, 1997]. Because these quasi-brittle materials do not contain the energy dissipative mechanisms that most ductile materials do, there is no method to re-balance the stresses induced by the microcrack stress concentrations. The *size effect* is a direct consequence of such high sensitivity of the response to microscale defects, as for example demonstrated in [Rinaldi et al., 2007, Genet et al., 2014].

When performing a fracture analysis, the rock heterogeneities can be modeled either explicitly or implicitly. Explicit models directly include inhomogeneities into the solution scheme. An example is lattice modeling, detailed in [Li, 2000], where a lattice of elements is used to represent a particle network connected by springs. The main downside to this approach is the small space and time scales required to directly resolve the microstructure. Implicit methods, on the other hand do not directly include microstructural details in the analysis and only incorporate their overall effect. As an example, the Weibull's weakest link model [Weibull, 1939, 1951] has proven very effective in capturing the size effect and stochastic variations in fracture response. We have used the Weibull model in the context of an interfacial damage model to capture statistical fracture response of rock, in hydraulic fracturing [Abedi et al., 2016], fracture under dynamic compressive loading [Abedi et al., 2017a], and in fragmentation studies [Abedi et al., 2017b, Clarke et al., 2017]. However, the Weibull model only provides a phenomenological characterization of fracture strength and lacks the direct connection to material microstructure that homogenization approaches provide, as discussed next.

Homogenization approaches derive macroscopic properties such as elastic moduli by solving the underlying problem in a *Volume Element* (VE). Similar approaches can also be used to calibrate certain fracture models, see for example [Taylor et al., 1986, Homand-Etienne et al., 1998, Shao and Rudnicki, 2000, Lu et al., 2013]. A *Representative Volume Element* (RVE) is a smaller subset of a larger domain that is still considerably larger than the microscale features in question. In order to simulate the macroscopic response of the material, the RVE must contain a large number of micro-heterogeneities such that the statistical response calculated from the RVE approaches the homogeneous macro response of the domain. Two problems with the use of RVEs in fracture analysis are the losses of spatial inhomogeneity and sample to sample variations. On the other hand, *Statistical Volume Elements* (SVEs) are VEs that are small enough to main both such variabilities. For example, SVEs are used for statistical analysis of elastic [Baxter and Graham, 2000, Tregger et al., 2006, Segurado and LLorca, 2006]

and fracture response [Koyama and Jing, 2007]. Moreover, we formulated SVEs for rock fracture in [Clarke and Abedi, 2017] and by using SVE-based homogenized properties, in [Clarke et al., 2017] we demonstrated the necessity of incorporating inhomogeneity in fracture strength; specifically we showed that a homogeneous fracture strength field predicted nonphysical sudden and spatially ubiquitous fragmentation patterns.

For real materials, incorporating randomness of strength in angle is also paramount, as materials fail based on specific spatial and angular weaknesses within the material. If the angle of loading of the material changes, so too does the behavior of the material. For rock, bedding planes make both elastic and fracture properties highly anisotropic. There have been two main approaches to model macroscopic anisotropies in rock fracture properties; Pietruszczak and Mroz [2000], Pietruszczak et al. [2002] added a second order so-called microstructure tensor to a stress-based general failure criterion for rock. On the other hand, in [Pietruszczak and Mroz, 2001, Lee and Pietruszczak, 2008, Shi et al., 2016] the parameters of well-known failure criteria such as Mohr-Coulomb or Hoek-Brown [Hoek and Brown, 1980] are made angle-dependent.

In this work, we extend our previous formulations of SVE for microcracked material [Clarke and Abedi, 2017, Clarke et al., 2017] by including the randomness in angle. We follow the second aforementioned approach, in that the parameters of a failure criterion, tensile strength in the context of a Mohr-Coulomb model herein, are made angle-dependent. The derivation of tensile strength follows the approach in [Acton et al., 2018], where a uniaxial stress load is applied at arbitrary directions around an SVE. To show the importance of considering this randomness in angle, two microcrack distributions, one uniform in angle, and another biased towards a specific angle, are used in our numerical analyses.

2 FORMULATION

In this section, a scheme is formulated which derives an analytic/computational representation of the microcrack distribution of a rock structure and its fracture strength. Subsection one shows how the RVE domain is developed with microcrack distribution. Subsection two then defines the SVE processing of the domain. Subsection three then details the fracture strength calculations performed within each SVE. Finally, a description of the *asynchronous Spacetime Discontinuous Galerkin* (aSDG) method is given, which is used to perform dynamic fracture simulations for the given rock domains.

2.1 *RVE Characterization*

A valid *representative volume element* (RVE) of a given rock structure must be large enough to properly represent the large number of micro-heterogeneities caused by microcracks in the rock structure, while still being sufficiently smaller than the overall macroscale structure. As the size of the volume element decreases, the meso-scale RVE approaches the *statistical volume element* (SVE) regime. The RVE domain size must represent the inhomogeneous fracture strength field at the macroscale based on the statistics of cracks in the RVE in the microscale.

For this paper, the RVE is represented by a rectangular 32-meter by 32-meter domain. Two different micro crack distributions were created within the domain via a take-and-place algorithm which generates the cracks and ensures no crack intersections. The microcrack length for both distributions is assumed to follow a Weibull distribution. For one distribution, the crack angle distribution follows a uniform distribution between 0 and 2π. The second domain contains an angularly-biased crack distribution to show the importance of introducing randomness of strength in angle direction, which without this randomness creates an unrealistic fracture response.

2.2 *SVE Characterization*

Within a given macroscale domain, a target domain is selected to analyze. This target domain is chosen as the RVE of the macro domain. To properly represent the microcrack distribution within the target domain RVE, smaller *statistical volume elements* (SVEs) are defined, within which the fracture strength of the rock is processed. The properties used to describe the SVE are the characteristic length of the macroscale domain length, L_M, the microscale heterogeneity average length l_m, and the characteristic size of the SVE, L_{SVE}. The characteristic size of the SVE must be much smaller than the domain of interest ($L_{SVE} \ll L_M$). Also, the ratio of the SVE size to the average heterogeneity length, β=L_{SVE}/l_m, should be small enough that the SVE does not approach the RVE limit. As β approaches ∞, the SVE approaches this limit, and randomness is lost. This loss of randomness will lead to inaccurate homogeneous material properties within the rock domain. To show this loss of randomness, several SVE sizes will be shown in the Numerical Results section. While a more succinct description on the relative size requirements of an SVE are given by [Du and Ostoja-Starzewski, 2006], the preference is for the SVE size to be small enough to maintain spatial variability within the RVE realization, while not being so small that there are many empty SVES without microcracks. The SVE must contain enough micro-heterogeneities to provide a comprehensive representation of the domain. Figure 1 depicts the macro to micro length scale variables within a rectangular domain.

For this paper, the SVE is circular, with a diameter L_{SVE}. The target domain is stepped through one by one, with the step size, S, a function of the SVE size, $S = L_{SVE}/n$. The grid line spacing variable, n, is selected such that the SVEs overlap and provide a complete characterization of the target domain. The center points of these overlapping SVEs form a uniform grid which are the points used to calculate the minimum fracture strength of the field. The outer edges of the RVE form the outer edge of the SVE center-point grid, as shown in the following figure. The intersection of the cracks with the SVE and the calculation of fracture strength within the SVE are given in the next

section.

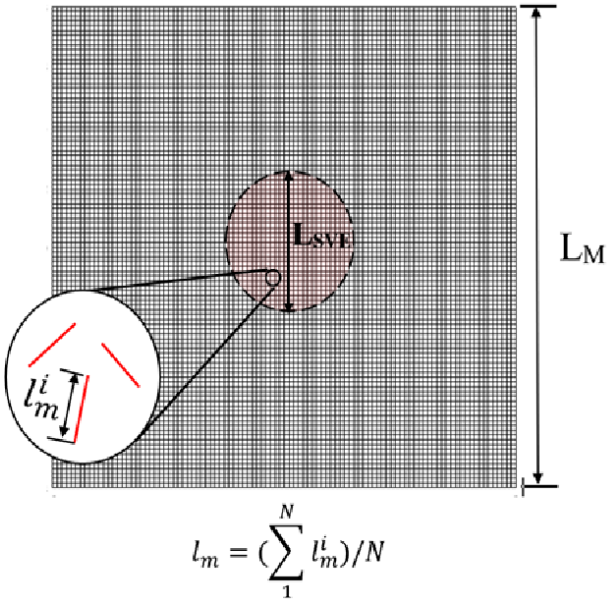

Figure 1: Macro- to microscale length scales relevant to SVE homogenization.

2.3 *Fracture Strength Calculations*

Once the SVE realizations have been created, the next step is to calculate the fracture strength that is assigned to the SVE over the entire range of loading angles. Within the SVE, both the cracks that are completely enclosed within the SVE and those that intersect the SVE are considered in computing an effective strength. If no crack intersects with the SVE, a maximum fracture strength is assigned based on a crack of minimum length. Figure 2 shows the intersection of cracks based on the SVE. The red lines indicate cracks that are not considered in calculating the fracture strength, while the blue lines indicate those that are considered. The effective length of the crack is considered to be the square root of the full crack length multiplied by the length intersecting the SVE.

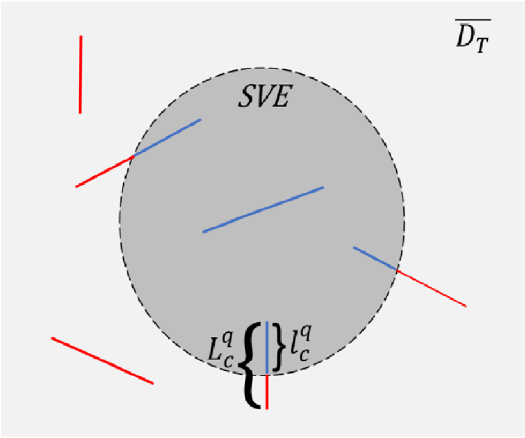

Figure 2: Cracks considered for strength calculation (Red Line considered crack segment external to SVE, Blue Line considered crack segment internal to SVE).

With a given crack of effective length a, the strength is calculated using *Linear Elastic Fracture Mechanics* (LEFM) principles. From this theory, upon the propagation of the first microcrack the SVE can be considered completely failed. The second assumption, as shown in [Nguyen et al., 2011], is that for quasi-brittle RVEs and SVEs with microcracks the load at which material response starts to deviate from linear elasticity is very close to the volume element's failure strength. Applying these assumptions to the model, the point of departure for linear elasticity is when the stress intensity factor for the most critical crack in the SVE reaches the fracture toughness. From this, the stress intensity factor is assumed to be approximated by that of a crack in an infinite domain. While this ignores crack interactions, this assumption is still believed to represent the inhomogeneity and anisotropy of macroscopic fracture field.

Therefore, applying the LEFM theory, the critical energy release rate G_C is used to calculate the fracture strength. The fracture strength is calculated over the entire range of potential loading angles. Figure 3 shows how the angle of loading, θ, changes for the calculation of the given strength. The loading angle at degree 0 is perpendicular to the crack direction, opening the crack and resulting in the angle of minimum fracture strength. Loading angles of 90 degrees are parallel to the crack tip, which will result in the maximum fracture strength for the given angle range.

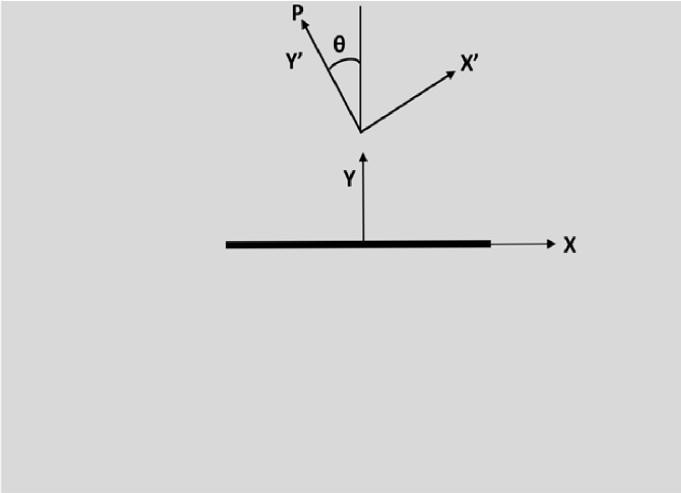

Figure 3: Angle of loading for crack strength calculation.)

This model results in a mixed-mode fracture strength calculation. From the applied traction loading, P, the resultant stress components σ_{yy} and σ_{xy} shown below are used to calculate the strength,

$$\sigma_{yy} = P\cos^2(\theta)$$
$$\sigma_{xy} = Pl_c\theta\cos\theta$$

For a plane strain problem, this results in the following:

$$(K_I^2 + K_{II}^2)\frac{(1-\nu^2)}{E} = G_C$$

If the Mode 1 stress intensity factor K_I is equal to $\sigma_{yy}\sqrt{\pi a}$ and Mode II stress intensity factor K_{II} equal to

$\sigma_{xy}\sqrt{\pi a}$, where a is equal to the effective length divided by two, then the fracture strength $\overline{S_{na}}$ is equal to

$$\overline{S_{na}} = \sqrt{\frac{G_C E}{(1-\nu^2)\pi a}} \frac{1}{|\cos\theta|} \tag{1}$$

As stated previously, the minimum strength occurs as θ approaches 0, while the maximum strength under loading occurs as θ approaches 90 degrees. The maximum strength automatically assigned to each SVE that does not contain a crack is equivalent to the strength at angle θ equal to zero degrees with the absolute minimum crack length a that is processed. This process is repeated over each crack contained within each SVE, and the minimum strength retained within each SVE. After calculating the minimum fracture strength for each SVE within the entire RVE domain, a field of minimum fracture strengths is created that represents the effects of the micro-heterogeneities on the given rock structure. This strength field and more for a given RVE is discussed in the next section.

2.4 *aSDG Method*

The asynchronous spacetime discontinuous Galerkin finite element method, as formulated for elastodynamic problem in [Abedi et al., 2006b] and extended for h-adaptive simulations in spacetime [Abedi et al., 2006a], is used to simulate the fracture of the heterogeneous domain. The method utilizes discontinuous basis functions across the element boundaries, and directly discretizes spacetime using nonuniform grids that satisfy a special causality constraint [Abedi et al., 2004]. Unique properties, such as a local and asynchronous solution scheme, arbitrarily high and local temporal order of accuracy, and linear solution scaling with number of elements, results in the ability to accurately and efficiently capture complex fracture patterns using a crack tracking technique [Omidi et al., 2015]. The resulting solution is both mesh independent and can accommodate crack propagation in any direction. Therefore, the aSDG method is optimal for rock fracture simulations.

3 NUMERICAL RESULTS

The domain used to calculate the statistical fracture strength is rectangular, centered at $x_{center} = (0,0)$ as shown in Figure 4. This domain, $\bar{D}$ spans 32 length units in both $\vec{x}$ and $\vec{y}$ directions, respectively, i.e. the domain spans from $x \in \bar{D} = [-16,-16]$ to $[16,16]$.

In order to generate the microcrack domain, as stated in Section 2, a Weibull distribution is assumed for the crack length and two different angle distributions are used for this work. The first angle distribution is uniform, between $[0, 2\pi]$, and has no angular bias. For the Weibull distribution, the *Weibull shape parameter* $m = 4$, *Weibull minimum value* $\gamma = 0.0755885$ m, and *Weibull scale* $\eta = 0.137259$ m are used to define the crack length distribution. For both the non-biased and biased angular distribution, the choice of Weibull parameters results in a mean crack length of 0.2 m with a standard deviation is 0.035 m. A minimum allowable crack length is set to 0.02 m, which thus becomes the minimum length for calculating the maximum strength, noted as the hydrostatic strength of the rock. The anisotropic crack distribution is biased to produce crack angles uniformly between -25 and -15 degrees, *i.e.,* this corresponds to a uniform distribution with the mean and span values of -20 and 10 degrees, respectively. Referring to convention used for defining of the orientation-dependent tensile strength, *cf.* Eq. (1), this implies that homogenized strengths should also be at their weakest at this angle range. Moreover, the angles $\pm$ 90 degrees from the crack angle, that is 65 to 75 degrees (-115 to -105 degrees), are expected to have the highest strengths, mainly determined by the largest strength corresponding to the minimum allowable crack length. The material properties are: Young's modulus $E = 65$ GPa, mass density $\rho = 2600$ kg/m^3, and Poisson's ratio $\nu = 0.3$. The critical energy release rate, G_C, in Eq. (1) is chosen such that the mean value of fracture strength is equal to 2 MPa. All the following strength results are reported in the MPa unit.

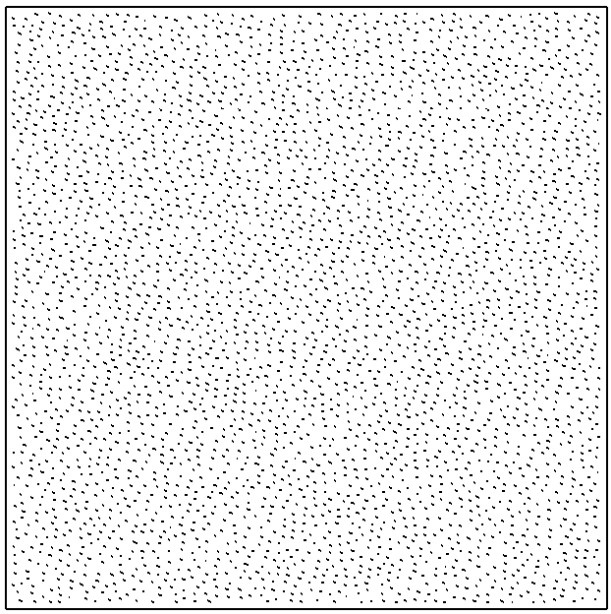

Figure 4: Example domain with distributed cracks.

3.1 *Angular Unbiased*

For the given angular unbiased crack distribution, the random fracture strength field was analyzed using several different SVE sizes. The given SVE sizes, denoted L_{SVE}, are 1, 2, 4, and 8 m. The loading angle, θ, was varied from $[0, \pi]$. The fracture strength was calculated for each crack within each SVE and the minimum fracture strength at each loading angle was determined within each SVE over the $[0, \pi]$ span. The angular spacing selected to calculate the minimum fracture strength was five degrees. The following figure shows how the random field varied based on angle for a selected 4x4 SVE.

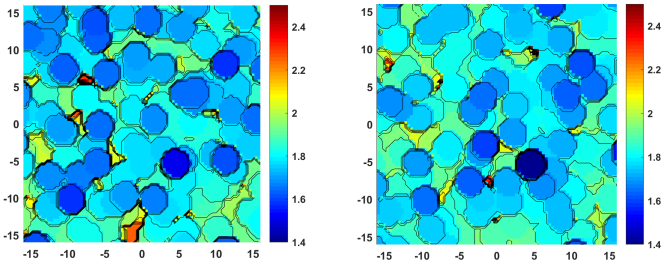

(a) 0 Deg Loading Angle (b) 30 Deg Loading Angle

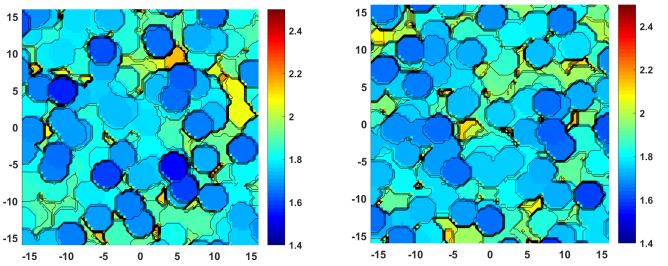

(c) 60 Deg Loading Angle (d) 90 Deg Loading Angle

Figure 5: Random fracture strength fields for four loading angles in non-biased domain.

The circular contours in Figure 5 are a result of the SVE shape chosen. For an angular unbiased mesh, the fracture strength distribution is truly random. At different loading angles, different SVEs within the RVE are more likely to fail than the others. Figure 6 shows the angular modulus, which is defined within each SVE as the fracture strength at a specific angle divided by the mean of the fracture strength over all angles. This plot shows how the strength changes at five different points in the mesh. The coordinates of these fives points in meters are $[-8.-8]$,$[8,8]$,$[-8,8]$,$[8,-8]$, and $[0,0]$. There is no clear trend for each of the five SVEs centered at these points.

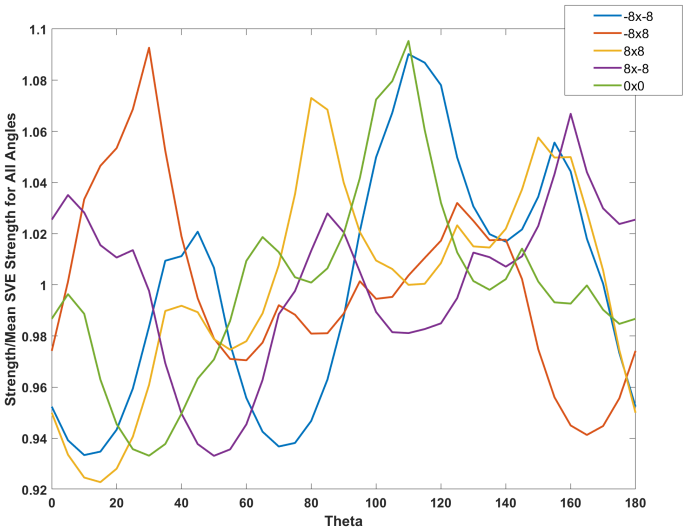

Figure 6: Fracture strength trend at five points in angular non-biased RVE with changing load angle.

Also, if the domain is truly unbiased by crack angle, then the fracture strength probability should be roughly equivalent over the entire loading angle span. From Figure 7, the probability density function follows this trend exactly. Therefore, it is confirmed that the crack angle field follows the uniform distribution exactly. A kernel smoothing function estimate is used to produce this plot using the uniaxial fracture strength data.

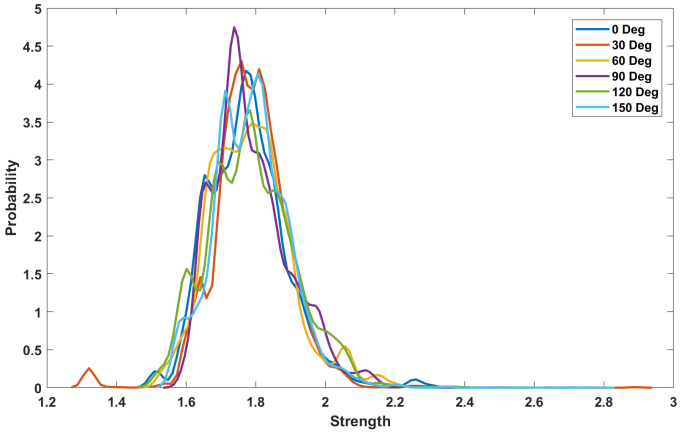

Figure 7: Probability density functions: $L_{SVE} = 4$, load angle comparison for $[0, \pi]$ span.

Rather than changing the loading angle, Figure 8 shows how the SVE size changes the random fields using the same loading angle, $\theta = 0$ degrees. The 1x1 SVE is very noisy, as it contains many SVEs without any cracks intersecting at all. Conversely, the 8x8 SVE is approaching a limit of grid coarseness such that it is approaching a homogeneous condition that does not properly model the true inhomogeneous fracture behavior of the rock.

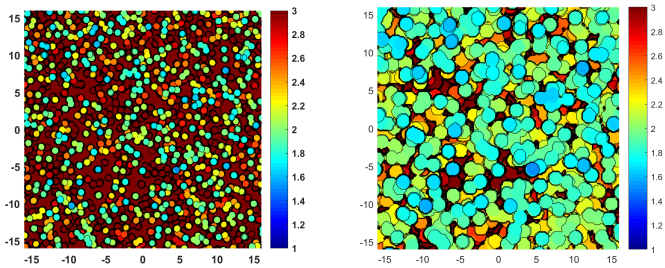

(a) $L_{SVE} = 1$ (b) $L_{SVE} = 2$

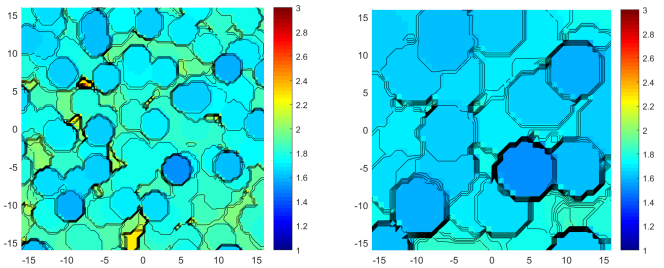

(c) $L_{SVE} = 4$ (d) $L_{SVE} = 8$

Figure 8: Random fracture strength fields for four SVE sizes at the same loading angle.

This size effect, caused by an increasing SVE size, can be seen in the following probability density function plot. In Figure 9, the probability is shown in the y-axis, while the strength is in the x-axis. As the SVE size increases,

the homogeneity of the random fracture strength field increases, as shown by the increasing probability and decrease of the width of the *probability density function* (PDF). For an SVE that is too small, the probability density function greatly decreases. The increased number of SVEs with no crack modeled within creates a split peak since these SVEs are assigned a maximum fracture strength, and the width of the PDF is large.

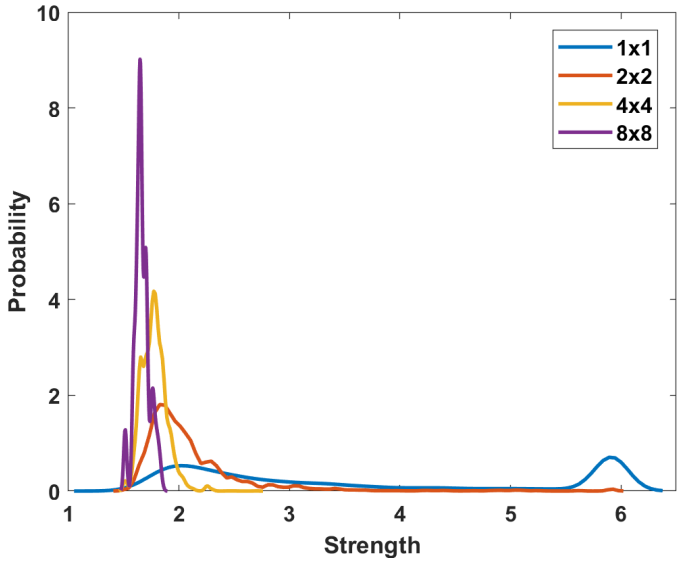

Figure 9: Probability density functions: SVE size comparison.

3.2 *Angular Biased*

While the angular unbiased domain shows true randomness, the biased crack domain is created such that all crack angles fall between -25 and -15 degrees. One realistic example of a biased cracks occurs in modeling bedding planes in sedimentary rock. The loading angle θ which would create the maximum stress field (i.e. the field of minimum fracture strength is perpendicular to the crack, *i.e.,* at angles -20 $\pm$ 90 = 70 and -110 degrees. The figure below shows the fracture strength for angles spanning from 70 to 160 degrees. The 70 degree load angle maintains an extremely high strength because the angle of loading is parallel to the crack. As the angle is increased, the strength steadily decreases until reaching a minimum strength at 160 (*i.e.,*-20) degrees. Without considering this fracture strength variation in angle, an inaccurate fracture strength could be assigned to the material.

Similar to that shown for the non-biased domain, five points with coordinates in meters ([$-8.$ -8],[$8, 8$],[$-8, 8$],[$8, -8$], and [$0, 0$]) were analyzed to show how the strength changes based on the angle. As expected, the lowest strength is observed for the direction of cracks around -20 degrees (that is 160 degrees), while the maximum strength is normal to this direction at around 70 degrees. This figure shows that at each point, the same trends hold due to the biased crack angles. For the biased mesh, it does not matter where samples are taken from as the same trend holds. This is due to the high anisotropy of fracture strength.

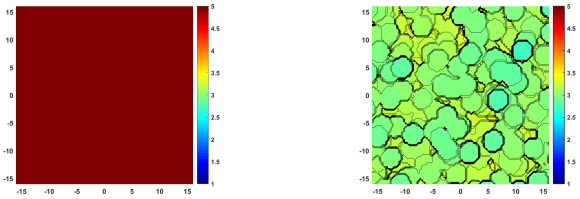

(a) 70 Deg Loading Angle (b) 100 Deg Loading Angle

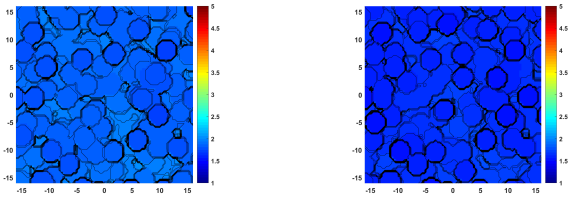

(c) 130 Deg Loading Angle (d) 160 Deg Loading Angle

Figure 10: Random fracture strength fields for four loading angles in -20 degree biased domain.

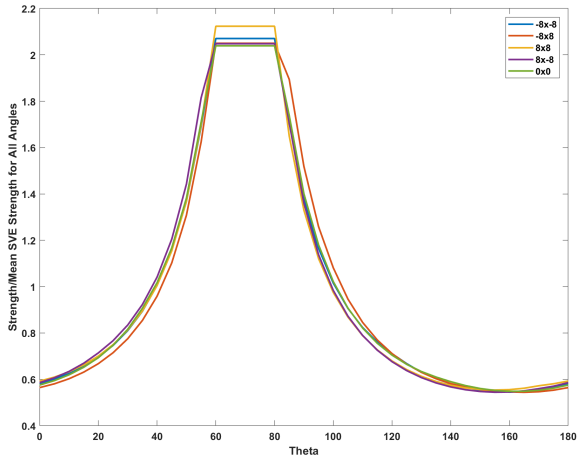

Figure 11: Fracture strength trend at five points in angular biased RVE with changing load angle.

Whereas before there was an equal probability to have an SVE that fails at a different angle, the PDF in Figure 12 for the sampled biased RVE does not follow this trend. As one gets closer to the location of lowest strength (160 degrees), the mean value decreases and the PDF shrinks (lower variations). Also, the PDF for the high strength angle of 60 degrees (close to the maximum expected strengths at 70 degrees) is low meaning that it has the highest deviation from the mean. Clearly, the mean for this angle of loading is the highest among the angles sampled. The size effect still holds for both domains as shown in Figure 13; however, the biased domain does not contain the split peak for the smallest SVE size. This is because the 0 degree loading angle is close to lowest strength angle of -20 degrees, so the entire domain has a near-homogeneous low strength value.

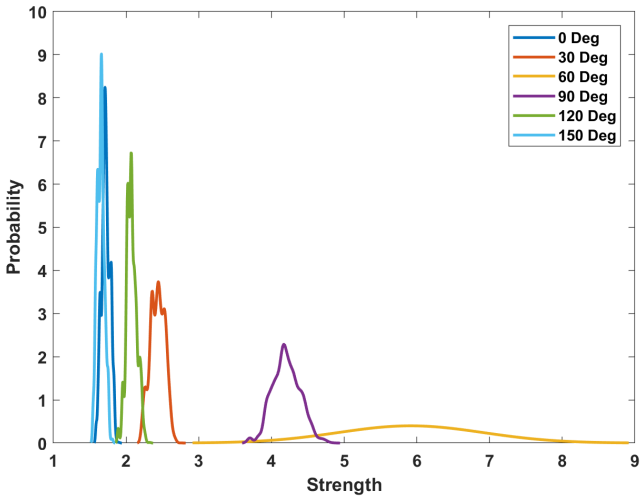

Figure 12: Probability density functions: $L_{SVE} = 4$, load angle comparison for $[0, \pi]$ span.

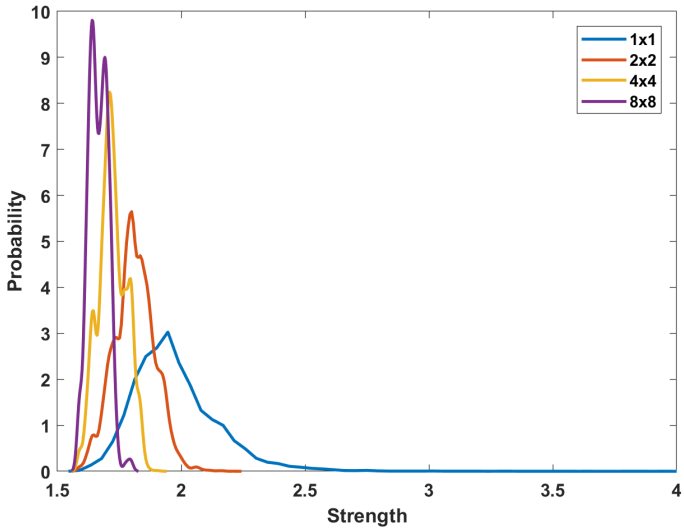

Figure 13: Probability density functions: SVE size comparison for angular biased domain.

3.3 *Dynamic Simulation of Random Fracture Strength Rock Domains*

The asynchronous spacetime discontinuous Galerkin finite element (aSDG) method was used to solve several dynamic fracture solutions using the given two differing random fields. This numerical scheme, implemented in C++, utilizes the aforementioned features in the Formulation section as well as advanced adaptive operations in spacetime to capture complex fracture patterns by a crack tracking adaptive scheme. The crack path is independent from a particular discrete mesh lay-out and accommodates crack propagation in any desired direction, a feature important for the anisotropic random field shown here.

Figures 14 and 15 show fracture patterns for non-angular biased and angular-field fracture strength fields under a spatially uniform and temporally increasing stress field. The description of the initial conditions and boundary conditions that can generate such s stress field (before the nucleation of the first macroscopic crack) is provided in [Abedi et al., 2017b]. From the angular-biased solution, it can be seen that the cracks all propagate in the direction of angular bias, *i.e.,* the original direction of microcracks. The density of nucleated and propagated cracks is higher for the angular-biased fracture field; *cf.* Figure 15. This would have resulted from the direct numerical simulation of the domains with explicit representation of all microcracks; since all would have been oriented close to -20 degrees, they would have extended along this direction under a spatially uniform and temporally increasing hydrostatic tensile field. The reduced interaction of the cracks, compared to the case with random orientation of microcracks, would have resulted in a higher density of propagated cracks. As mentioned, our results for the homogenized fields exhibit the same behavior in these figures.

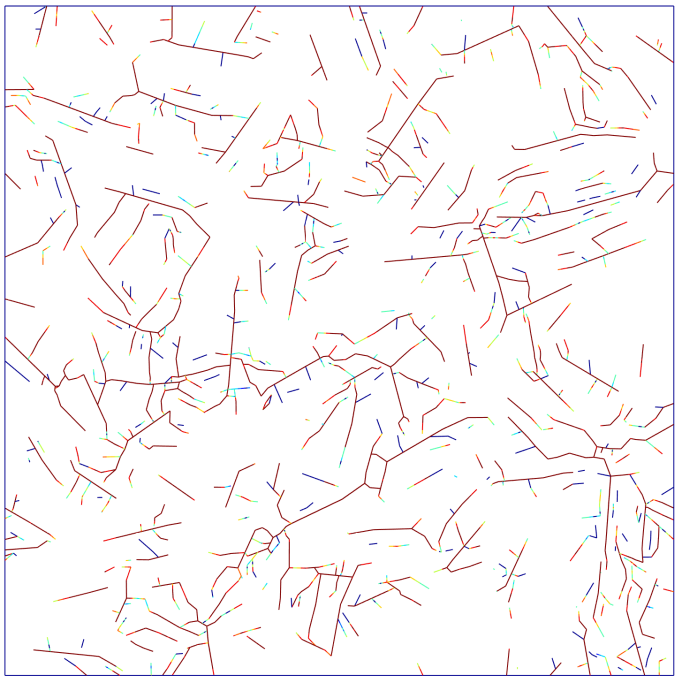

Figure 14: Dynamic simulation of non-angular biased random fracture field.

As stated previously, for a given SVE size, the larger the SVE, the less realistic the fracture response. An SVE size L_{SVE} of 4 was chosen for this analysis, which provided enough heterogeneity in the solution. If the rock domain contains anisotropy, however, the spatial inhomogeneity is not enough to properly model the complex crack field. Without modeling the angular dependence of the field, weaker planes within the rock are not considered. Therefore, depending on the angle of loading, different crack paths are preferred, and complex fracture patterns are formed. This differs greatly from the biased domain, wherein only one path is generally preferred. This confirms the importance of including angular variability when modeling quasi-brittle materials such as rock.

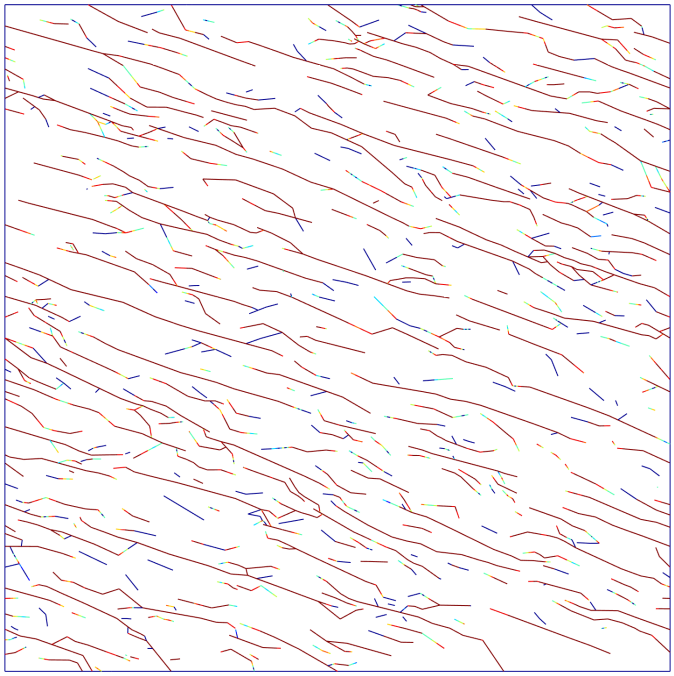

Figure 15: Dynamic simulation of angular-biased random fracture field.

4 CONCLUSIONS

In order to include the effects of weaker planes within a brittle material such as rock, there is great importance in including both spatial and angular variability when calculating the random fracture strength field within a domain. In this work, two microcrack distributions were developed to demonstrate the importance of considering the given angular variability within the structure of the rock domain. An SVE approach was chosen to model the random fracture field. Each intersecting crack located within the SVE was analyzed, and the minimum overall fracture strength was assigned to that SVE. This process was repeated over a range of loading angles. The center points of the SVE formed a uniform grid which could then be sent to a dynamic analysis to simulate rock with its inherent fracture strength inhomogeneity and anisotropy. Selecting the proper size for the SVE was important, as given an SVE size too small provided a noisy domain, which can lead to a split peak in the probability density function of the solution and the noise can impact the solution of the dynamic fracture analysis. Meanwhile, an SVE size too large approaches the RVE limit, leading to an unrealistic homogeneity in the solution, which also provides an unrealistic dynamic fracture analysis.

The results from both the uniformly distributed domain and biased microcrack domain fracture analysis showed the importance of including angular variability. The angular-biased domain cracks grew only along one primary direction, corresponding to the in-situ bedding plane direction, under a hydrostatic tensile stress field. An anisotropic rock bed has weaker and stronger planes, and fractures should grow along the path of least fracture strength. The dynamic solution of these domains indicates a complex crack pattern can be expected for a problem like this, which would be missed without including this angular variability. Otherwise, the material would inaccurately assumed to be equally likely to fail in the same direction under any loading condition.

There are a few items to improve upon this work. First, a Weibull distribution was used to model the crack length distribution. A Pareto distribution may be more accurate in modeling the microcrack distribution for a quasi-brittle material, as shown in [Daphalapurkar et al., 2011]. The effect of using this distribution or other distributions instead of a Weibull will be investigated in a future paper. Second, this paper only takes into account uniaxial tensile strength for these simulations. A future improvement will take into account shear and compressive strengths as well for any angle of loading. We studied the effect of randomness on fracture pattern for uniaxial compressive testing in [Abedi et al., 2017a] and our model captured fracture along $\pm(45^\circ \pm \phi/2)$ where ϕ is the friction angle, with respect to the loading direction. While these results qualitatively agree with other numerical and experimental observations [Tang et al., 2000, Teng et al., 2004, Li and Tang, 2015, Dinç and Scholtès, 2017, Bahmani et al., 2018, Rangari et al., 2018] we plan to extend our model for such compressive fracture studies but when fracture strength is no longer isotropic. This will be of great practical importance as rock often fractures in compressive or shear modes. Third, we aim to the obtain the anisotropic covariance function for the fracture strength field and use in realizing statistically consistent random fields by the *Karhunen-Loève* (KL) method [Karhunen and Selin, 1960, Loéve, 1977]. This in turn enables treating the rock fracture problem as a *stochastic partial differential equation* (SPDE) which can be solved efficiently with methods detailed in [Ghanem and Spanos, 1991].

REFERENCES

R. Abedi, R. B. Haber, S. Thite, and J. Erickson. An h–adaptive spacetime–discontinuous Galerkin method for linearized elastodynamics. *Revue Européenne de Mécanique Numérique (European Journal of Computational Mechanics)*, 15(6):619–42, 2006a.

R. Abedi, O. Omidi, and P.L. Clarke. Numerical simulation of rock dynamic fracturing and failure including microscale material randomness. In *Proceeding: 50th US Rock Mechanics/Geomechanics Symposium*, Houston, Texas, USA, 2016. ARMA 16-0531.

R. Abedi, R.B. Haber, and A. Elbanna. Mixed-mode dynamic crack propagation in rocks with contact-separation mode transitions. In *Proceeding: 51th US Rock Mechanics/Geomechanics Symposium*, San Francisco, California, USA, 2017a. ARMA 17-0679.

Reza Abedi, Shuo-Heng Chung, Jeff Erickson, Yong Fan, Michael Garland, Damrong Guoy, Robert Haber, John M. Sullivan, Shripad Thite, and Yuan Zhou. Spacetime meshing with adaptive refinement and coarsening.

In *Proceedings of the Twentieth Annual Symposium on Computational Geometry*, SCG '04, pages 300–9, Brooklyn, New York, USA, June 9-11 2004. ACM.

Reza Abedi, Robert B. Haber, and Boris Petracovici. A spacetime discontinuous Galerkin method for elastodynamics with element-level balance of linear momentum. *Computer Methods in Applied Mechanics and Engineering*, 195:3247–73, 2006b.

Reza Abedi, Robert B. Haber, and Philip L. Clarke. Effect of random defects on dynamic fracture in quasi-brittle materials. *International Journal of Fracture*, 208(1-2): 241–268, 2017b.

K.A. Acton, S.C. Baxter, B. Bahmani, P.L. Clarke, and R. Abedi. Voronoi tessellation based statistical volume element characterization for use in fracture modeling. *Computer Methods in Applied Mechanics and Engineering*, 2018. In Press.

A. Al-Ostaz and I. Jasiuk. Crack initiation and propagation in materials with randomly distributed holes. *Engineering Fracture Mechanics*, 58(5-6):395–420, 1997.

Bahador Bahmani, Philip L. Clarke, and Reza Abedi. A bulk damage model for modeling dynamic fracture in rock. In *Proceeding: 52nd US Rock Mechanics/Geomechanics Symposium*, Seattle, Washington, USA, 2018. ARMA 18-151-0228-0826 (9 pages).

S. C. Baxter and L. L. Graham. Characterization of random composites using moving-window technique. *Journal of Engineering Mechanics*, 126(4):389–397, 2000.

P.L. Clarke and R. Abedi. Fracture modeling of rocks based on random field generation and simulation of inhomogeneous domains. In *Proceeding: 51th US Rock Mechanics/Geomechanics Symposium*, San Francisco, California, USA, 2017. ARMA 17-0643.

P.L. Clarke, R. Abedi, B. Bahmani, K.A. Acton, and S.C. Baxter. Effect of the spatial inhomogeneity of fracture strength on fracture pattern for quasi-brittle materials. In *Proceedings of ASME 2017 International Mechanical Engineering Congress & Exposition IMECE 2017*, Tampa, Florida, USA, 2017. IMECE2017-71515.

N.P. Daphalapurkar, K.T. Ramesh, L. Graham-Brady, and J.F. Molinari. Predicting variability in the dynamic failure strength of brittle materials considering pre-existing flaws. *Journal of the Mechanics and Physics of Solids*, 59(2):297–319, 2011.

Özge Dinç and Luc Scholtès. Discrete analysis of damage and shear banding in argillaceous rocks. *Rock Mechanics and Rock Engineering*, pages 1–18, 2017.

Xiangdong Du and Martin Ostoja-Starzewski. On the scaling from statistical to representative volume element in thermoelasticity of random materials. *Networks and heterogeneous media*, 1(2):259, 2006.

M. Genet, G. Couegnat, A.P. Tomsia, and R.O. Ritchie. Scaling strength distributions in quasi-brittle materials from micro- to macro-scales: A computational approach to modeling nature-inspired structural ceramics. *Journal of the Mechanics and Physics of Solids*, 68(1):93–106, 2014.

R. Ghanem and P.D. Spanos. *Stochastic finite elements: a spectral approach*. Springer-Verlag, 1991.

E. Hoek and T. Brown. *Underground Excavations in Rock*. Geotechnics and foundations. Taylor & Francis, 1980.

F. Homand-Etienne, D. Hoxha, and J.F. Shao. A continuum damage constitutive law for brittle rocks. *Computers and Geotechnics*, 22(2):135–151, 1998.

Kari Karhunen and Ivan Selin. *On linear methods in probability theory*. Rand Corporation, 1960.

Tomofumi Koyama and Lanru Jing. Effects of model scale and particle size on micro-mechanical properties and failure processes of rocks—a particle mechanics approach. *Engineering Analysis with Boundary Elements*, 31(5): 458–472, 2007.

J Kozicki and J Tejchman. Effect of aggregate structure on fracture process in concrete using 2D lattice model. *Archives of Mechanics*, 59(4-5):365–84, 2007.

Y.-K. Lee and S. Pietruszczak. Application of critical plane approach to the prediction of strength anisotropy in transversely isotropic rock masses. *International Journal of Rock Mechanics and Mining Sciences*, 45(4):513–23, 2008.

Gen Li and Chun-An Tang. A statistical meso-damage mechanical method for modeling trans-scale progressive failure process of rock. *International Journal of Rock Mechanics and Mining Sciences*, 74:133–150, 2015.

Jia Li. Debonding of the interface as 'crack arrestor'. *International Journal of Fracture*, 105(1):57–79, 2000.

M. Loéve. *Probability theory*. Springer, New York, 1977.

Y.L. Lu, D. Elsworth, and L.G. Wang. Microcrack-based coupled damage and flow modeling of fracturing evolution in permeable brittle rocks. *Computers and Geotechnics*, 49:226–44, 2013.

Vinh Phu Nguyen, Oriol Lloberas-Valls, Martijn Stroeven, and Lambertus Johannes Sluys. Homogenization-based multiscale crack modelling: From micro-diffusive damage to macro-cracks. *Computer Methods in Applied Mechanics and Engineering*, 200(9):1220–1236, 2011.

Omid Omidi, Reza Abedi, and Saeid Enayatpour. An adaptive meshing approach to capture hydraulic fracturing. In *The 49th US Rock Mechanics/Geomechanics Symposium*, San Francisco, California, USA, 2015. ARMA 15-572.

S. Pietruszczak and Z. Mroz. Formulation of anisotropic failure criteria incorporating a microstructure tensor. *Computers and Geotechnics*, 26(2):105–112, 2000.

S. Pietruszczak and Z. Mroz. On failure criteria for anisotropic cohesive-frictional materials. *International Journal for Numerical and Analytical Methods in Geomechanics*, 25(5):509–524, 2001.

S. Pietruszczak, D. Lydzba, and J.F. Shao. Modelling of inherent anisotropy in sedimentary rocks. *International Journal of Solids and Structures*, 39(3):637–648, 2002.

Sachin Rangari, K Murali, and Arghya Deb. Effect of mesostructure on strength and size effect in concrete under compression. *Engineering Fracture Mechanics*, 2018.

A. Rinaldi, D. Krajcinovic, and S. Mastilovic. Statistical damage mechanics and extreme value theory. *International Journal of Damage Mechanics*, 16(1):57–76, 2007.

Javier Segurado and Javier LLorca. Computational micromechanics of composites: The effect of particle spatial distribution. *Mechanics of Materials*, 38(8):873–883, 2006.

J.F. Shao and J.W. Rudnicki. A microcrack-based continuous damage model for brittle geomaterials. *Mechanics of Materials*, 32(10):607–619, 2000.

Xiangchao Shi, Xu Yang, Yingfeng Meng, and Gao Li. An anisotropic strength model for layered rocks considering planes of weakness. *Rock Mechanics and Rock Engineering*, 49(9):3783–92, 2016.

CA Tang, LG Tham, PKK Lee, Y Tsui, and H Liu. Numerical studies of the influence of microstructure on rock failure in uniaxial compression - part II: constraint, slenderness, and size effect. *International Journal of Rock Mechanics and Mining Sciences*, 37(4):571–583, 2000.

Lee M. Taylor, Er-Ping Chen, and Joel S. Kuszmaul. Microcrack-induced damage accumulation in brittle rock under dynamic loading. *Computer Methods in Applied Mechanics and Engineering*, 55(3):301 – 320, 1986.

JG Teng, WC Zhu, and CA Tang. Mesomechanical model for concrete. part II: applications. *Magazine of Concrete Research*, 56(6):331–345, 2004.

Nathan Tregger, David Corr, Lori Graham-Brady, and Surendra Shah. Modeling the effect of mesoscale randomness on concrete fracture. *Probabilistic Engineering Mechanics*, 21(3):217–225, 2006.

W. Weibull. A statistical theory of the strength of materials. *R. Swed. Inst. Eng. Res.*, page Res. 151, 1939.

W. Weibull. A statistical distribution function of wide applicability. *Journal of Applied Mechanics*, 18:293–297, 1951.

Xiaolei Yin, Wei Chen, Albert To, Cahal McVeigh, and Wing Kam Liu. Statistical volume element method for predicting microstructure–constitutive property relations. *Computer methods in applied mechanics and engineering*, 197(43-44):3516–29, 2008.